CMS Physics Analysis Summary

Contact: cms-pag-conveners-exotica@cern.ch 2011/10/31

Search for new physics with long-lived particles decaying to photons and missing energy

The CMS Collaboration

Abstract

A search for long-lived neutral particles decaying into a photon and invisible particles is performed. In the context of gauge mediated supersymmetry with the lightest neutralino as the next-to-lightest supersymmetric particle and the gravitino as the lightest supersymmetric particle, the neutralino can decay into a gravitino and a photon with a nonzero lifetime. The impact parameter of the photon relative to the beam-beam collision point can be reconstructed using converted photons. The method is sensitive to lifetimes of the order of $\mathcal{O}$(0.1 ns). The data sample corresponds to an integrated luminosity of 2.1 ± 0.1 fb^{-1} recorded in the first part of 2011 by the CMS experiment at the LHC at $\sqrt{s}$ = 7 TeV. The search is performed using events containing photons, missing transverse energy and jets. Upper limits at the 95% confidence level are presented on the cross section for such particles from pair-production, each of which decays into a photon and invisible particles.

New heavy particles with long lifetimes are predicted in many models of physics beyond the Standard Model (SM), like Hidden Valley [1] or supersymmetry (SUSY) with gauge-mediated breaking [2–7]. Such particles may be neutral and decay into photons and invisible particles. Their lifetime is essentially a free parameter of the model. For sufficiently high decay lengths $\mathcal{O}(1\text{ m})$, measurement of shower direction [8] or time-of-flight [9] with the electro-magnetic calorimeter can be used to identify such decays.

In this note, we devise a new method which is sensitive to much shorter lifetimes for decay lengths of $\mathcal{O}(1\text{ cm})$. Capitalizing on the large amount of material in the CMS tracker, we use photons that undergo conversion into e^+e^- pairs. The tracks of the electrons can be precisely reconstructed and used to calculate the photon trajectory and, in particular, the impact parameter of the photon with respect to the interaction point.

We search for a signature of a photon with significant impact parameter in association with missing transverse energy. As a signal benchmark, we use the classic gauge-mediated SUSY model SPS8 [10, 11]. Figure 1 shows a typical production diagram. Assuming R parity is conserved, SUSY particles are produced in pairs and decay into SM particles and the lightest neutralino ($\tilde{\chi}_1^0$). The neutralino decays into a photon and a gravitino, the lightest SUSY particle in this model, which escapes the detector, leading to apparent missing energy E_T^{miss}. Moreover, in all relevant models, the $\tilde{\chi}_1^0$ is produced in association with high p_T jets. We consider neutralino decay lengths between $c\tau = 2$ cm and $c\tau = 25$ cm, corresponding to the lifetime in the range of $\mathcal{O}(0.1\text{ ns})$ to $\mathcal{O}(1\text{ ns})$.

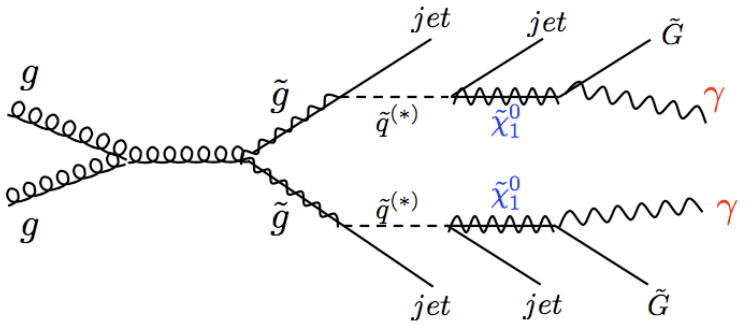

Figure 1: Feynman diagram of $\tilde{\chi}_1^0$ pair production and $\tilde{\chi}_1^0 \to \gamma + \tilde{G}$ decay.

The data sample was collected in 2011 by the CMS detector at the LHC for pp collisions at a center-of-mass-energy of 7 TeV, corresponding to an integrated luminosity of 2.1 fb^{-1}. The analysis strategy is to select events with a diphoton final state, and then to examine the impact parameter of each single photon for the displaced photon signal. Missing transverse energy (E_T^{miss}) and the presence of jets are also required. The background is estimated using a low E_T^{miss} control sample. Upper limits on the cross section for pair-production of $\tilde{\chi}_1^0$s, each of which decays into a photon and invisible particles, are set as the function of the $\tilde{\chi}_1^0$ lifetime.

A detailed description of the CMS detector can be found elsewhere [12]. The detector's central feature is a superconducting solenoid providing a 3.8 T axial magnetic field along the beam direction. Charged particle trajectories are measured by a silicon pixel and strip tracker system, covering $0 \leq \phi \leq 2\pi$ in azimuth and $|\eta| < 2.5$, where the pseudo-rapidity is defined as $\eta = -\ln\tan\theta/2$, and θ is the polar angle with respect to the counterclockwise beam direction. A lead-tungstate crystal electromagnetic calorimeter (ECAL) and a brass/scintillator hadron calorimeter (HCAL) surround the tracker volume. For the barrel calorimeter ($|\eta| < 1.479$), the modules are arranged in projective towers. Muons are measured in gas detectors embedded

in the steel return yoke of the magnet. The detector is nearly hermetic, allowing for reliable measurement of E_T^{miss}.

The data were recorded using the CMS two-level trigger system. This analysis selects events with at least two photons. A diphoton trigger is required with ECAL energy thresholds ranging from 32 GeV (22 GeV) to 40 GeV (28 GeV) for the leading (sub-leading) photon, over the course of the data taking period. To be on the plateau of trigger efficiency, the offline analysis selects events with at least two photons with $E_T > 45$ GeV (30 GeV) for the leading (sub-leading) photon in the event. The data sample is used both for the selection of signal candidates and for control samples used for background estimation.

The PYTHIA6 event generator [13] has been used to simulate SUSY signal events. In particular, we have generated SUSY GMSB signal datasets in the benchmark model [10]. In this sample every event has two neutralinos, each of which has a mass of 140 GeV and a specific lifetime. The signal selection efficiency can depend on the $\tilde{\chi}_1^0$ mass, but it is a negligible effect in this analysis. Each of the neutralinos decays to a photon and a gravitino. The CMS detector response has been fully simulated using the CMSSW program which is also used for collision data. The same software has been also used to reconstruct the physics objects so that all features of the detector are included in the signal acceptance calculations.

The pile-up conditions will affect the trigger and conversion reconstruction efficiencies. The generated pile-up distribution in the Monte Carlo samples has been reweighted to mimic the 2011data taking conditions.

The photon candidates are reconstructed from clusters of energy in the ECAL. At least one photon candidate with transverse energy $E_T > 45$ GeV and reconstructed in the ECAL barrel region is required. Its ECAL cluster shape must be consistent with that expected from a photon, and the ratio of the energy detected in the HCAL behind the photon shower cannot exceed 5% of the ECAL energy. To suppress hadronic jets faking photon candidates, we require the latter to be isolated in the tracker, ECAL and HCAL. A cone of $\Delta R = \sqrt{(\Delta\eta)^2 + (\Delta\phi)^2} = 0.4$ is constructed around the candidate's direction, and the scalar sums of transverse energies of tracks and calorimeter deposits within this ΔR are determined, after excluding the contribution from the candidate itself. The isolation sums are required to be $< 0.006 \cdot E_T + 4.2$ GeV, $< 0.0025 \cdot E_T + 2.2$ GeV, and $< 0.001 \cdot E_T + 2.0$ GeV, for the ECAL, HCAL and tracker, respectively. To distinguish photons from electrons, we require that the hit patterns in the pixel detector be consistent with a track from an electron (pixel match). Converted photons are recovered by requiring the pixel matched electron to be consistent with a conversion.

Photon-like signals that have the same definition as photons but do not satisfy the isolation requirements are referred to as "fake photons". These objects, predominantly jets that fragmented into neutral particles like π^0, are used for the background estimation.

Jets are reconstructed from energy deposits in the calorimeters using the anti-k_T clustering algorithm [14]. The energies of these jets are corrected for the p_T of the charged tracks reconstructed in the tracker [15]. At least two jets are required with $p_{T1} > 80$ GeV and $p_{T2} > 50$ GeV and $|\eta| \leq 2.6$.

Missing transverse energy is calculated from calorimeter energy deposits. It is corrected using tracking information for energy missed due to incomplete calorimeter measurements of muons and charged hadrons energies, especially for soft tracks that do not reach the calorimeters [16]. An E_T^{miss} threshold of 30 GeV is set to distinguish the signal from the background.

The CMS tracker, based on silicon technology, was designed to provide robust and precise

reconstruction of charged-particle momenta in the high occupancy environment of LHC collisions. Achieving this goal inevitably led to a substantial amount of tracker material. As a result, a large fraction of photons convert into e^+e^- pairs, called "photon conversions", while traversing the tracker. Conversions can be used to obtain the photon direction. By extrapolation along the momentum direction from the conversion vertex back to the beam line, we can calculate the impact parameter of the displaced photons (Fig. 2). If the $\tilde{\chi}_1^0$ has a non-zero lifetime, the decay photons can originate in the tracker volume rather than at the primary vertex and will point away. Quantitively these photons can have non-zero impact parameters (IP), which can be the signature for the long-lived $\tilde{\chi}_1^0$ signal.

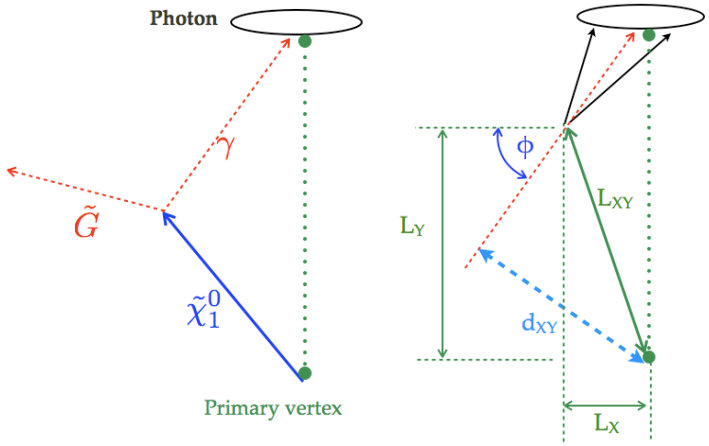

Figure 2: (a) The decay $\tilde{\chi}_1^0 \to \gamma + \tilde{G}$ as seen in the CMS tracker; (b) diagram of the photon conversion into an e^+e^- pair, showing the reconstruction of the impact parameter.

The transverse impact parameter d_{XY} is the distance of closest approach of the photon trajectory to the beam line in the transverse plane. The longitudinal impact parameter d_Z is the distance from the chosen primary vertex to the Z position where d_{XY} is calculated (Equation 1). The photon trajectory is defined as a straight line from the conversion vertex along the conversion momentum.

$$\begin{aligned} d_{XY} &= -L_X \cdot \sin\phi + L_Y \cdot \cos\phi \\ d_Z &= L_Z - \frac{L_X \cdot p_X + L_Y \cdot p_Y}{p_T} \cdot \frac{p_Z}{p_T} \end{aligned} \tag{1}$$

Equation 1 shows d_{XY} and d_Z in terms of the vector between the conversion vertex and the primary vertex (L), and the polar angle ϕ of the conversion momentum vector p in azimuth. The momentum p is calculated by the vector summation of the e^+e^- pair momenta at the conversion vertex.

Because the conversion vertex has zero invariant mass, the e^+e^- tracks should be parallel in momentum so that the kinematic constraint of θ and ϕ of the track momenta can be applied to select conversion tracks, and the conversion vertex can be fitted using the kinematic constraint. Three reconstruction algorithms are used: the "tracker-only" [17, 18], the "ECAL-seeded" [19], and the "Gaussian Sum Filter" (GSF) electron [20]. The tracker-only algorithm selects conversion track pairs from all reconstructed tracks, with the kinematic constraint, and fits the conversion vertex; the ECAL-seeded algorithm takes the energy deposit of conversion tracks

in the ECAL as seeds and then extrapolates back to the tracker to fit the conversion tracks and vertices; the GSF electron algorithm follows a similar procedure to the tracker-only algorithm but uses GSF electrons to find the track pairs. The conversions from these three algorithms are merged and the duplicates are removed. Among the reconstructed conversion tracks the one with the largest number of hits is kept if its χ^2 probability is not significantly worse than the others (χ^2 probability should be greater than 10^{-6}). Otherwise the track with the highest χ^2 probability is kept and the others are removed. To select the conversions, the two opposite-signed tracks both need at least five valid hits and the conversion vertex requires a valid fit with χ^2 probability $> 5 \times 10^{-4}$.

In high luminosity conditions, multiple collisions give multiple primary vertices. The true primary vertex has a large deviation in the longitudinal direction but much less uncertainty in the transverse direction. To be robust against the pile-up conditions, the transverse impact parameter (d_{XY}) w.r.t the transverse position of the the beam line is used in this analysis. To illustrate the d_{XY} signature, its distribution in data with $E_T^{miss} > 30$ GeV is compared with a Monte Carlo sample with $\tilde{\chi}_1^0$ lifetime $c\tau$ = 5 cm, as shown in Fig. 3. The requirement that d_{XY} be larger than 0.6 cm defines the signal region. This value for d_{XY} is derived by optimizing the expected limits on the production cross section. As seen in Fig. 3, one event passes all selection criteria. The Monte Carlo sample is normalized to the integrated luminosity and 7.79 events pass all selections.

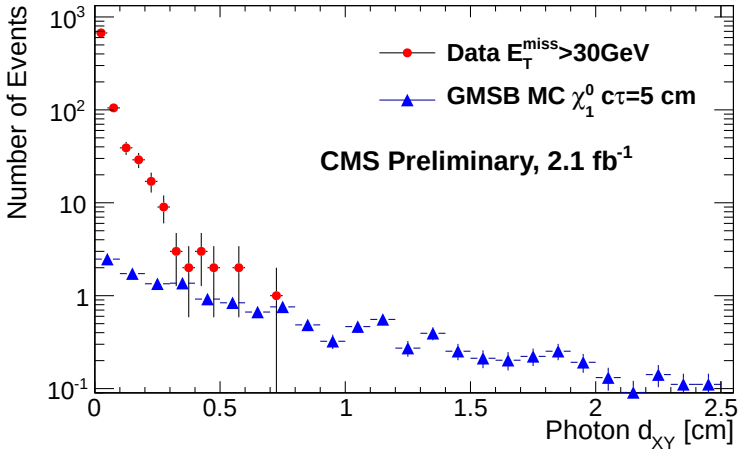

Figure 3: d_{XY} distribution for data with $E_T^{miss} > 30$ GeV compared with signal simulation for $c\tau$ = 5 cm normalized to the integrated luminosity of the data.

The effect of the event selection is illustrated in Table 1 for the $c\tau$ = 5 cm sample. Of the 45,057 events which were simulated, 711 events remain after all the cuts, for an overall event selection efficiency of 1.58%. Efficiencies for four neutralino lifetimes are given in Table 2. On average, the signal event selection efficiency is about 1% to 2% after all the above trigger requirements and the selection criterial are applied.

Because of the γ's and jets in the final state, the background is due to single-γ-plus-jets events and QCD multi-jets events with no true large E_T^{miss}. In single-γ-plus-jets events, the true energetic photons are the final state ones. In QCD multi-jets events, the jets can be misidentified as photons. The $\tilde{\chi}_1^0 \rightarrow \gamma + \tilde{G}$ decay has two signatures: E_T^{miss} from the unseen $\tilde{G}$ and large

Table 1: Signal selection flow for $c\tau$ = 5 cm.

Selection	Events in Monte Carlo
Total	45057
DiPhoton trigger	39988
Photon $E_T > 45$ GeV and $E_T > 30$ GeV	37398
Any ECAL barrel photon $E_T > 45$ GeV and Photon identification	27766
Jets $p_T > 80$ GeV and $p_T > 50$ GeV	26229
Conversion selection	1602
$E_T^{miss} > 30$ GeV	1542
$d_{XY} > 0.6$ cm	711

Table 2: Event selection efficiency vs $\tilde{\chi}_1^0$ lifetime.

$c\tau$ [cm]	2	5	10	25
Efficiency	0.921%	1.578%	1.797%	1.388%
Statistical errors	0.046%	0.059%	0.064%	0.055%

IP from the displaced photons. The strategy for determining the background is to use control samples which are kinematically similar to the candidate sample while having no real E_T^{miss}. The data with $E_T^{miss} < 20$ GeV are selected as such a control sample for the background estimation. The background is then estimated as the number of events with E_T^{miss} less than 20 GeV and satisfying all the other selection criteria.

To ensure the $E_T^{miss} < 20$ GeV region of data gives a correct estimation of the background, the d_{XY} distributions of fake photons and isolated photons are compared. Fake photons are defined as photon signatures that do not satisfy the isolation requirement. First, the fake photon d_{XY} distribution for events with $E_T^{miss} < 20$ GeV (background region) is normalized by the total number of conversions and compared with the d_{XY} distribution of fake photons in the $E_T^{miss} > 30$ GeV (signal region) (Fig.4a). Because the d_{XY} resolution is strongly dependent on the conversion vertex χ^2 probability, where worse χ^2 probability gives worse vertex position resolution, leading to worse d_{XY} resolution, the d_{XY} distribution in the low E_T^{miss} (background region) is re-weighted by the conversion vertex χ^2 probability of the signal region. Second, the d_{XY} distributions of isolated photons and fake photons in the low E_T^{miss} region are compared by normalizing the total number of conversions, also re-weighted by the conversion vertex χ^2 probability (Fig.4b). Agreement of the d_{XY} distributions of fake photons and isolated photons is observed, and thus we conclude that the d_{XY} distribution for $E_T^{miss} < 20$ GeV gives a good description of the background.

In Fig. 5 the d_{XY} distributions for the signal and background regions are shown. They are normalized to the same numbers of conversions and re-weighted by the conversion vertex χ^2 probability, to predict the number of background events. A requirement that $d_{XY} > 0.6$ cm is applied to the background region $E_T^{miss} < 20$ GeV, which extrapolated to the signal region, gives a total background of $0.78^{+1.25}_{-0.48}$ events.

Table 3 summarizes the systematic uncertainties affecting this study. To determine the uncertainty in the conversion reconstruction efficiency, we compared the predicted and observed numbers of conversions for $Z \to \mu\mu\gamma$ events. For photons with $E_T > 20$ GeV, a scale factor Data-MC of 0.87 ± 0.08 is derived. High E_T photons have a reconstruction efficiency of $7.0 \pm 0.5\%$ in the Drell-Yan to di-muon Monte Carlo samples, and the corresponding high E_T photon efficiency in the GMSB Monte Carlo samples is $6.0 \pm 0.7\%$, giving a $Z \to \mu\mu\gamma$-GMSB

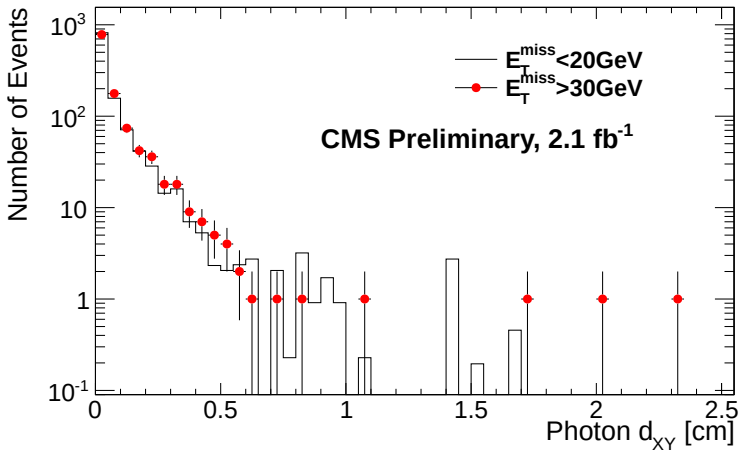

(a)

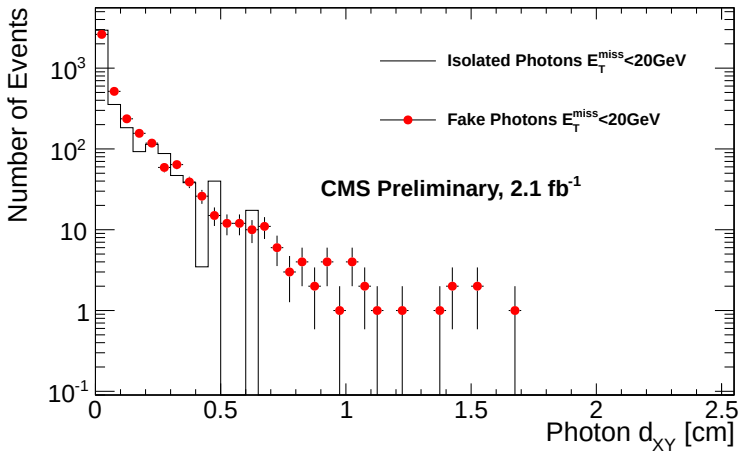

(b)

Figure 4: Photon d_{XY} comparison: (a) fake photon in background and signal region; (b) isolated and fake photon distributions in background region.

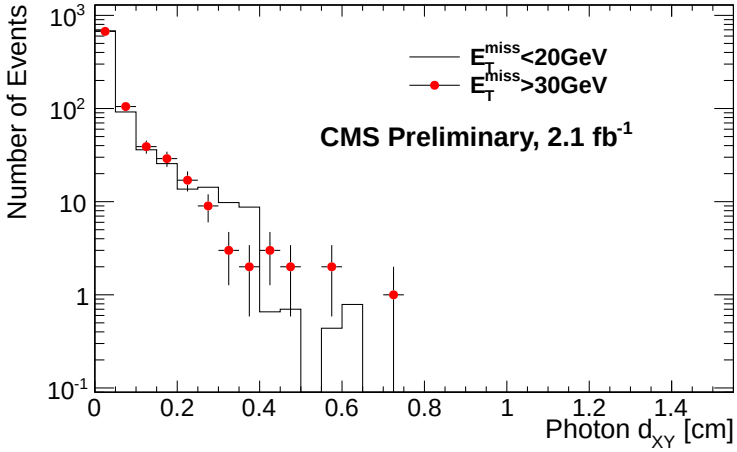

Figure 5: d_{XY} distribution: background region compared to the signal region.

scale factor of 1.16 ± 0.08. Taking into account the uncertainty in the conversion efficiency scale factor and the high E_T dependence, the uncertainty of conversion reconstruction is set to 20.6% for the signal region of interest.

The resolution of d_{XY} has been studied by comparing the d_{XY} resolution of $Z \to \mu\mu\gamma$ in Monte Carlo and data. A good agreement is observed. The d_{XY} resolution of 0.06 cm extracted from data gives less than 0.5% uncertainty for the signal selection.

Other sources of uncertainties include: integrated luminosity (4.5%); jet p_T/E_T^{miss} selection requirement and photon identification. The jet$/E_T^{miss}$ selection cut contributes with less than 0.5% to the total uncertainty [15, 16]. The photon identification efficiency is studied in [11] and includes the uncertainties from pile-up (2.5%), photon Data/MC scale measured in $Z \to ee$ data sample (2.6%) and photon-electron identification difference as studied in MC samples(0.5%). Other sources of uncertainties give negligible contribution to the systematic uncertainty. The total systematic uncertainty is set to 25%.

Systematics	Uncertainty (%)
Integrated luminosity	4.5
Jet p_T/E_T^{miss} energy scale	< 0.5
Pile-up	2.5
Photon identification Data/MC scale	2.6
Photon-electron difference	0.5
Conversion reconstruction efficiency	20.6
Photon d_{XY} resolution	< 0.5
Total	25

Table 3: Summary of systematic uncertainties.

One event with $d_{XY} = -0.74$ cm and $E_T^{miss} = 44.9$ GeV satisfying all the other selection criteria is observed. The estimated background is $0.78^{+1.25}_{-0.48}$ events. We determine the upper limits for the cross section for pair-production of $\tilde{\chi}_1^0$'s, each of which decays into one photon and invisible particles. A CLs limit setting method [21, 22] is employed using the log-normal uncertainties for the total background rate, to incorporate uncertainty in the total background rate, integrated luminosity, and total acceptance times efficiency. The observed 95% confidence level limits vary between 0.12 and 0.24 pb, depending on the $\tilde{\chi}_1^0$ lifetime (Table 4 and Fig. 6).

$c\tau$ [cm]	2	5	10	25
σ [pb] 95% C.L	0.24	0.14	0.12	0.16

Table 4: 95% C.L. upper limits on neutralino productions cross section as a function of neutralino lifetime.

In summary, the photon conversion impact parameter method has been applied for searching for new physics involving long-lived particles decaying into photons. By using a data-driven method to estimate the background, a search in the final state of γs, jets and missing transverse energy has been performed. Upper limits on the cross section for such particles from pair-production decaying into a photon and invisible particles are set as a function of the long-lived particle's lifetime.

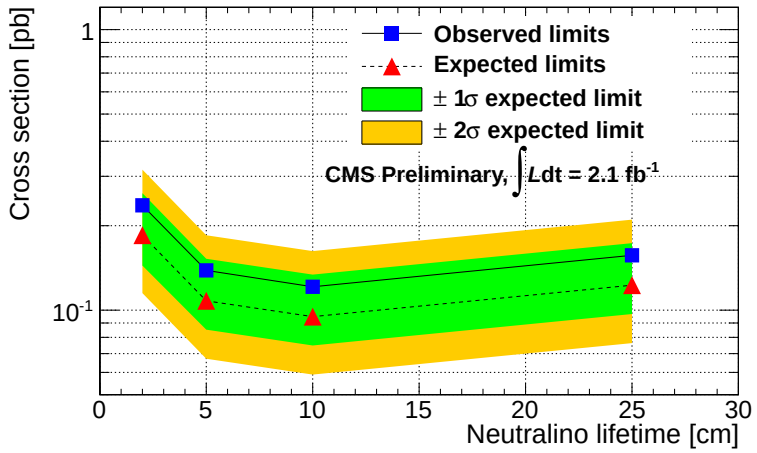

Figure 6: 95% C.L. upper limits on neutralino productions cross section as a function of neutralino lifetime.

References

[1] M. J. Strassler and K. M. Zurek, "Echoes of a hidden valley at hadron colliders", *Phys.Lett.* **B651** (2007) 374–379, arXiv:hep-ph/0604261. doi:10.1016/j.physletb.2007.06.055.

[2] L. M. Carpenter, "Surveying the Phenomenology of General Gauge Mediation", arXiv:0812.2051.

[3] A. Rajaraman, Y. Shirman, J. Smidt et al., "Parameter Space of General Gauge Mediation", *Phys.Lett.* **B678** (2009) 367–372, arXiv:0903.0668. doi:10.1016/j.physletb.2009.06.047.

[4] S. Abel, M. J. Dolan, J. Jaeckel et al., "Phenomenology of Pure General Gauge Mediation", *JHEP* **0912** (2009) 001, arXiv:0910.2674. doi:10.1088/1126-6708/2009/12/001.

[5] J. T. Ruderman and D. Shih, "General Neutralino NLSPs at the Early LHC", arXiv:1103.6083.

[6] P. Meade, M. Reece, and D. Shih, "Prompt Decays of General Neutralino NLSPs at the Tevatron", *JHEP* **1005** (2010) 105, arXiv:0911.4130. doi:10.1007/JHEP05(2010)105.

[7] P. Meade, M. Reece, and D. Shih, "Long-Lived Neutralino NLSPs", *JHEP* **1010** (2010) 067, arXiv:1006.4575. doi:10.1007/JHEP10(2010)067.

[8] D0 Collaboration Collaboration, "Search for long-lived particles decaying into electron or photon pairs with the D0 detector", *Phys.Rev.Lett.* **101** (2008) 111802, arXiv:0806.2223. doi:10.1103/PhysRevLett.101.111802.

[9] CDF Collaboration Collaboration, "Search for heavy, long-lived particles that decay to photons at CDF II", *Phys.Rev.Lett.* **99** (2007) 121801, arXiv:0704.0760. doi:10.1103/PhysRevLett.99.121801.

[10] B. Allanach, M. Battaglia, G. Blair et al., "The Snowmass points and slopes: Benchmarks for SUSY searches", *Eur.Phys.J.* **C25** (2002) 113–123, arXiv:hep-ph/0202233. doi:10.1007/s10052-002-0949-3.

[11] CMS Collaboration, "Search for Supersymmetry in Events with Photons, Jets and Missing Energy", *CMS Physics Analysis Summary* **SUS-11-009** (2011).

[12] CMS Collaboration, "The CMS experiment at the CERN LHC", *JINST* **0803** (2008) S08004. doi:10.1088/1748-0221/3/08/S08004.

[13] T. Sjostrand, S. Mrenna, and P. Z. Skands, "PYTHIA 6.4 Physics and Manual", *JHEP* **0605** (2006) 026, arXiv:hep-ph/0603175. doi:10.1088/1126-6708/2006/05/026.

[14] M. Cacciari, G. P. Salam, and G. Soyez, "The Anti-k(t) jet clustering algorithm", *JHEP* **0804** (2008) 063, arXiv:0802.1189. doi:10.1088/1126-6708/2008/04/063.

[15] CMS Collaboration, "Jet Performance in pp Collisions at $\sqrt{s}$=7 TeV", *CMS Physics Analysis Summary* **JME-10-003** (2010).

[16] CMS Collaboration, "MET Performance in pp Collisions at $\sqrt{s}$=7 TeV", *CMS Physics Analysis Summary* **JME-10-009** (2010).

[17] CMS Collaboration, "Tracking and Vertexing Results from First Collisions", *CMS Physics Analysis Summary* **TRK-10-001** (2010).

[18] CMS Collaboration, "Studies of Tracker Material", *CMS Physics Analysis Summary* **TRK-10-003** (2010).

[19] N. Marinelli, "Track finding and identification of converted photons", *CMS NOTE* **2006/005** (2006).

[20] J. B. M. Sani, M. Pieri, "Electron GSF Tracking Commissioning with first LHC Data", *CMS NOTE* **2010/038** (2010).

[21] A. L. Read, "Presentation of search results: The CL(s) technique", *J.Phys.G* **G28** (2002) 2693–2704. doi:10.1088/0954-3899/28/10/313.

[22] L. Moneta, K. Belasco, K. Cranmer et al., "The RooStats Project", *PoS* **ACAT2010** (2010) 057, arXiv:1009.1003. * Temporary entry *.